Middle-Late Permian mass extinction on land

Gregory J. Retallack†
Christine A. Metzger
Department of Geological Sciences, University of Oregon, Eugene, Oregon 97403-1272, USA

Tara Greaver
A. Hope Jahren
Department of Earth and Planetary Sciences, Johns Hopkins University, Baltimore, Maryland 21218, USA

Roger M.H. Smith
Department of Karoo Palaeontology, Iziko South African Museum, P.O. Box 61, Cape Town 8000, South Africa

Nathan D. Sheldon
Department of Geology, Royal Holloway University of London, Egham, Surrey TW20 OEX, England

ABSTRACT

The end-Permian mass extinction has been envisaged as the nadir of biodiversity decline due to increasing volcanic gas emissions over some 9 million years. We propose a different tempo and mechanism of extinction because we recognize two separate but geologically abrupt mass extinctions on land, one terminating the Middle Permian (Guadalupian) at 260.4 Ma and a later one ending the Permian Period at 251 Ma. Our evidence comes from new paleobotanical, paleopedological, and carbon isotopic studies of Portal Mountain, Antarctica, and comparable studies in the Karoo Basin, South Africa. Extinctions have long been apparent among marine invertebrates at both the end of the Guadalupian and end of the Permian, which were also times of warm-wet greenhouse climatic transients, marked soil erosion, transition from high- to low-sinuosity and braided streams, soil stagnation in wetlands, and profound negative carbon isotope anomalies. Both mass extinctions may have resulted from catastrophic methane outbursts to the atmosphere from coal intruded by feeder dikes to flood basalts, such as the end-Guadalupian Emeishan Basalt and end-Permian Siberian Traps.

Keywords: Permian, Triassic, extinction, paleosol, palynology, vertebrates.

INTRODUCTION

Carbon isotope chemostratigraphy is a method for international correlation of marked

carbon isotope excursions, which are interpreted as global perturbations in isotopic composition of atmospheric CO_2 (Jahren et al., 2001; Berner, 2002). The global marine negative $\delta^{13}C$ excursion at the Permian-Triassic boundary (Baud et al., 1989) was the first of at least four profound carbon-isotope excursions (Payne et al., 2004) within the first 6 m.y. of the Triassic Period (time scale of Gradstein et al., 2005). All four excursions have been found on land as well (Krull and Retallack, 2000), and confirm correlation of the Permian-Triassic boundary on land with the boundary-stratotype marine sequence in China (Retallack et al., 2005). By comparison, the Late Permian (Lopingian) atmospheric carbon dioxide record shows less variability in isotopic composition, with the next oldest carbon isotopic perturbation some 9 m.y. earlier (time scale of Gradstein et al., 2005) at the stratotype-marine Guadalupian-Lopingian (Middle-Late Permian) boundary (Wang et al., 2004). A carbon isotope excursion at a comparable stratigraphic position has been found at Graphite Peak in Antarctica (Krull and Retallack, 2000), and here we report additional end-Guadalupian carbon isotope excursions at Portal Mountain, Antarctica, and near Beaufort West in the Karoo Basin, South Africa. This advance in land-sea correlation of the Late Permian has implications for understanding Late Permian mass extinctions and environmental changes on land.

The end-Permian mass extinction was the greatest biotic crisis of the Phanerozoic, but an earlier end-Guadalupian mass extinction of marine invertebrates was comparable with end-Cretaceous mass extinction in the sea (Stanley and Yang, 1994; Wang et al., 2004). With our new chemostratigraphic correlation, we now

report both end-Guadalupian and end-Permian extinctions among fossil plants and vertebrates on land in Antarctica and South Africa (Fig. 1). Instead of a 9 m.y. decline in biodiversity on land to terminal Permian extinction (Benton et al., 2004; Ward et al., 2005), we demonstrate that terrestrial mass extinctions were abrupt, like those in the sea at the end of both the Guadalupian and Permian. Furthermore, our examination of end-Guadalupian paleosols and paleochannels in South Africa and Antarctica show striking similarities, indicative of excursions in soil erosion, stream stability, soil oxidation, mean annual temperature, and mean annual precipitation. The end-Guadalupian mass extinction was followed by landscape destabilization and warm-wet postapocalyptic greenhouse comparable to that already documented for the end-Permian mass extinction (Retallack et al., 2003, 2005; Ward et al., 2005; Sheldon, 2006).

MATERIALS AND METHODS

In November 2003, we measured a stratigraphic section and collected Late Permian fossil plants from the east ridge of Portal Mountain, southern Victoria Land, Antarctica (78.10784°S, 159.29979°E, 2107 m). Samples collected in tinfoil and plastic bags were analyzed for organic matter released by HCl and HF digestion, then combusted in sealed tubes with Cu, CuO, and Ag. Released CO_2 was purified cryogenically, and collected for $^{13}C/^{12}C$ measurement relative to Vienna Peedee belemnite using an Isoprime mass spectrometer at Johns Hopkins University.

South African paleosol data were obtained during November 2001 while examining the Beaufort Group along a transect through the
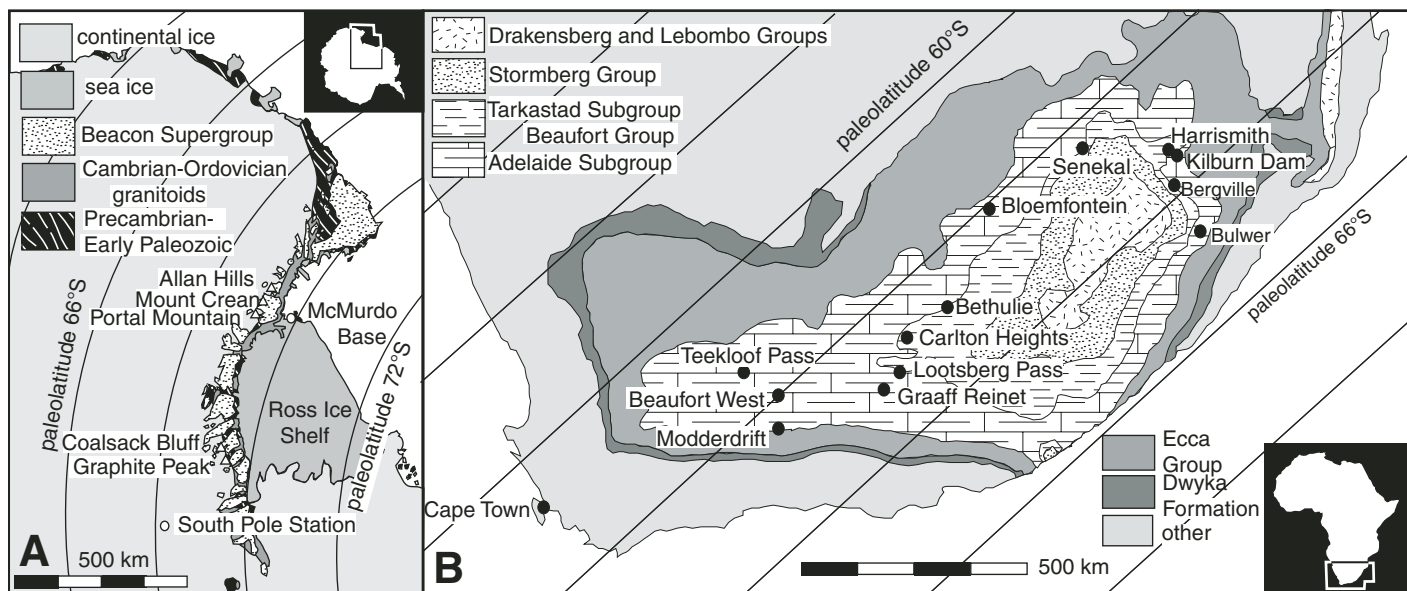
Figure 1. Localities examined on simplified geological maps of Antarctica (A) and South Africa (B), showing Late Permian paleolatitude.

lower Beaufort Group from the Ecca-Beaufort contact near Modderdrift in the Prince Albert district to the top of Teekloof Pass in the Fraserburg district (Retallack et al., 2003; Retallack, 2005a). South African palynological data and ranges are from Falcon (1975a, 1975b), Anderson (1977), Stapleton (1978), MacRae (1988), Horowitz (1990), and Steiner et al. (2003) and have been updated to current taxonomic usage (for stratigraphic levels, synonymies, and taxonomic authorship details, see GSA Data Repository item[1]). South African vertebrate data are from Ward et al. (2005), with minor corrections for misnumbering and duplication of names. South African carbon isotope data are from both organic carbon (Keith, 1969; Faure et al., 1995; MacLeod et al., 2000; Ward et al., 2005) and from phosphatic tusks of *Diictodon* and *Lystrosaurus* (Thackeray et al., 1990). The tusk data have been replotted with newly determined stratigraphic levels based on subsequent biostratigraphic refinement (Rubidge, 1995) and reexamination of museum records (see GSA Depository item [footnote 1]).

INTERNATIONAL CHEMOSTRATIGRAPHIC CORRELATION

Our new carbon isotopic analyses of the section at Portal Mountain, Victoria Land,

Antarctica, show two negative carbon isotopic anomalies, one of −2.9‰ low in the section and another of −1.1‰ $\delta^{13}C_{kerogen}$ high in the section (Figs. 2 and 3). The carbon isotopic composition of pedogenic carbonate and of therapsid tooth enamel from South Africa also shows two negative carbon isotope anomalies, one of −7.7‰ in the middle of the sequence and another of −2.8‰ $\delta^{13}C_{apatite}$ high in the sequence (Fig. 2). These two anomalies correlate with end-Guadalupian and end-Permian carbon isotope anomalies for the following reasons.

End-Guadalupian and end-Permian negative isotopic anomalies appear to be global (Fig. 2). The end-Permian anomaly is known from 55 sites worldwide (tabulated by Retallack and Krull, 2006). The end-Guadalupian anomaly is known from 17 sites worldwide (Table 1). Additional end-Cisuralian and several Early Triassic negative carbon isotope anomalies (265.5, 250.5, 247.6, and 245 Ma in Fig. 2) also appear to be global and may have had similar causes and consequences (Payne et al., 2004; Retallack, 2005a; Retallack et al., 2005).

Correlation is partly based on pattern recognition from comparably analyzed long sections, including marine sections spanning the Dorashamian and Dzhulfian Stages, which are considered to be equivalent to the Wuchaipingian and Changsingian of Chinese stratotype sections (Baud et al., 1996). The end-Guadalupian marked negative anomaly is followed by Late Permian (Wuchaipingian-Changsingian) isotopic stability, then four quickly successive isotopic anomalies of the Early Triassic (Payne et al., 2004). The various sections studied for carbon

isotopic composition plotted in Figure 2 all have different meter scales, reflecting variations in local subsidence rate, yet the proportional stratigraphic spacing of the carbon isotope anomalies is strikingly similar. This pattern persists through documented increases in sediment accumulation rate following the end-Permian mass extinction in South Africa (Retallack et al., 2003), Antarctica (Retallack and Krull, 1999), and Australia (Retallack, 1999). Such consistently aligned carbon isotope anomalies may represent a succession of globally synchronous events unequally spaced in time and of unequal magnitude.

Local biostratigraphic, pedostratigraphic, and sedimentologic evidence from Portal Mountain in Antarctica also constrains international correlation of carbon isotope excursions. Fossil leaves of *Glossopteris*, and the distinctive chambered root of the same plant named separately as *Vertebraria*, known to have been extinguished at the end of the Permian (Retallack et al., 2005), range through to the upper isotopic excursion (Fig. 3). The lower isotopic excursion corresponds to other range truncations, especially of *Gangamopteris* and *Palaeovittaria*, which are characteristic of Early and Middle Permian sequences, including the Ecca Group of South Africa (Anderson and Anderson, 1995), Talchir and Karharbari Formations of India (Chandra and Singh, 1996), and Greta Coal Measures of eastern Australia (Retallack, 1980). In contrast, our collections from the upper Weller Coal measures on Portal Mountain resemble Late Permian (Lopingian) *Glossopteris* floras, characterized by fine-meshed, medium to small leaves, and reproductive
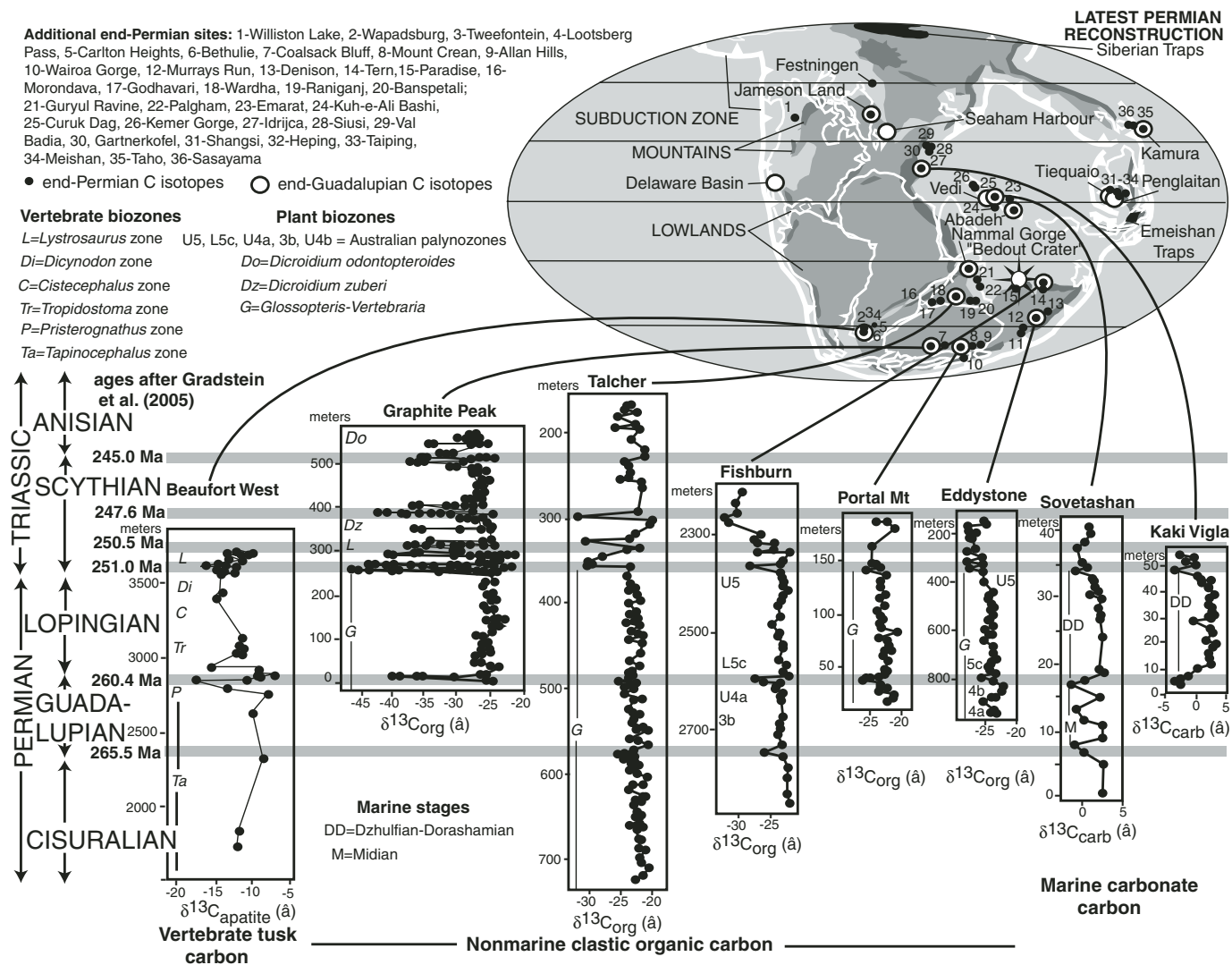
Figure 2. Carbon isotopic records showing both end-Guadalupian and end-Permian carbon cycle crises. Published and new records (see GSA Depository item [text footnote 1]) have been scaled to equalize local sediment accumulation rates and show correlations within the time scale of Gradstein et al. (2005). Carbon isotope anomalies are in both marine carbonate (Sovetashan and Kaki Vigla) and in nonmarine organic matter (other sites).

structures such as *Dictyopteridium*, *Rigbya*, *Senotheca,* and *Squamella* in Antarctica (upper Weller Coal Measures at Mount Crean, Buckley Formation at Graphite Peak and Coalsack Bluff, Mount Glossopteris Formation of Horlick Mountains: Retallack et al., 2005), Australia (Newcastle Coal Measures; Retallack, 1980), India (Raniganj Formation: Tewari, 1996), and South Africa (Estcourt Formation: Anderson and Anderson, 1995; Gastaldo et al., 2005). Antarctic palynology gives only broad constraints because the entire Weller Coal Measures is assigned to the undivided *Protohaploxypinus* zone, which correlates with Australian Middle Permian palynozone 4 (Kyle, 1977; Isbell and Cuneo, 1996), but also ranges into

Late Permian palynozone 5 (Isbell et al., 1999). *Dulhuntyispora* is a key element of Australian Late Permian (stage 5) palynofloras, but is not found in the Antarctic Permian, presumably for ecological reasons, because it is missing from undoubtedly Late Permian palynofloras in Antarctica (Truswell, 1980; Retallack et al., 2005; Collinson et al., 2006). Finally, the earliest Triassic of Antarctica is also indicated by berthierine-nodular paleosols (Dolores pedotype) and braided stream deposits above the last coal (Retallack et al., 2005), also seen at Portal Mountain (Fig. 3).

Local biostratigraphic and geochronological constraints in South Africa demonstrate that the two carbon isotopic excursions occurred there

during the end-Guadalupian and end-Permian. In terms of vertebrate biozones (Rubidge, 1995), the upper isotopic excursion is near the base of the *Lystrosaurus* zone, and the lower isotopic excursion is in the lower *Pristerognathus* zone to upper *Tapinocephalus* zone. In terms of South African palynology (Anderson, 1977), the isotopic excursions fall above and below palynological stages 6–7, which are together correlative with stage 5 of Australian palynofloras (Truswell, 1980). The upper isotopic excursion is within the Permian-Triassic boundary transition for palynofloras, with its distinctive fungal-algal spike (Steiner et al., 2003). No megafossil floras are known from the *Tapinocephalus* zone in South Africa, but
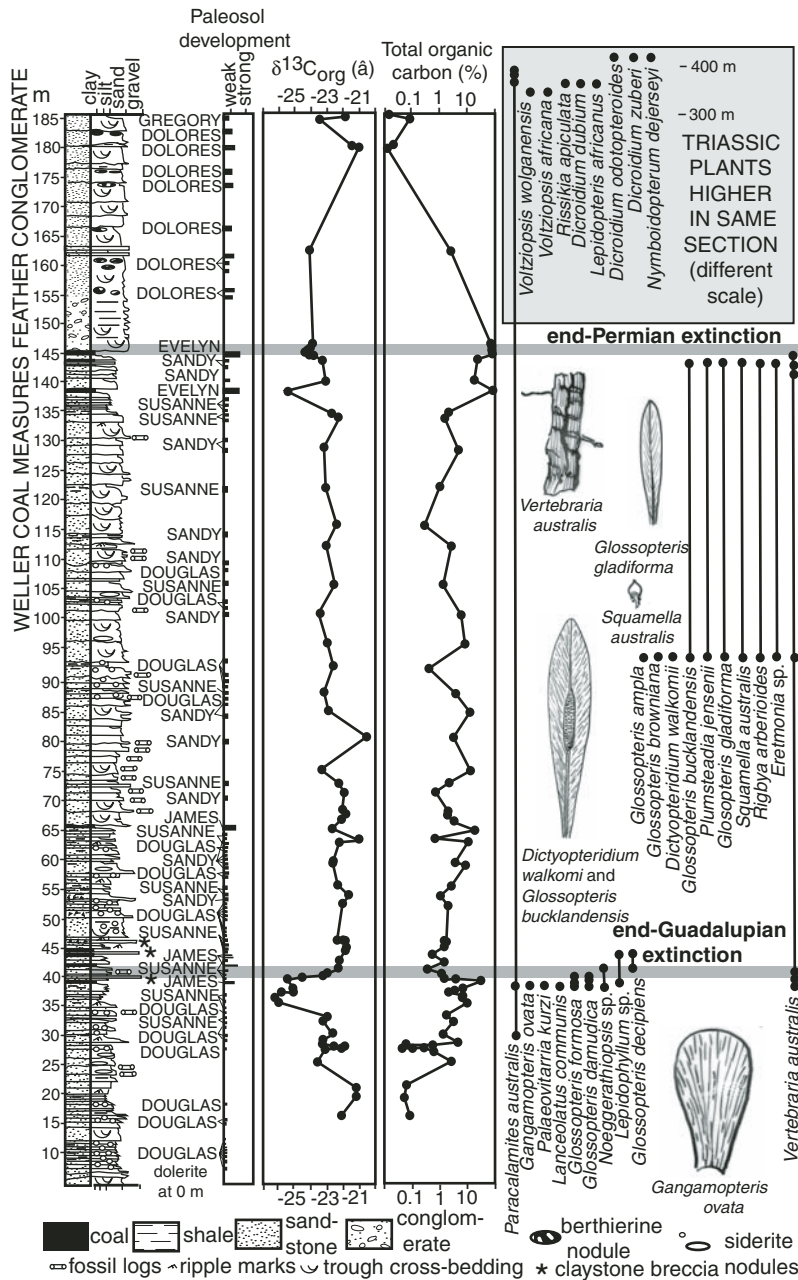
Figure 3. Late Permian rocks and fossils at Portal Mountain, Antarctica. Left to right: graphic log of lithologies, identified paleosol pedotypes and their degree of development (Retallack et al., 2005), new analyses of carbon isotopic composition of organic matter and of total organic content (see GSA Depository item [text footnote 1]), and stratigraphic ranges of newly collected fossil plants.

carbon isotope excursion in the Karoo Basin is at the Permian-Triassic boundary (Ward et al., 2005). Linear extrapolation from 251 Ma for that boundary (following Gradstein et al., 2005) back to radiometrically dated ashes in the Ecca Group and Dwyka Tillite (Ghosh et al., 1998; Bangert et al., 1999; Stollenhofen et al., 2000) suggest that the carbon isotope excursion following the end of the *Tapinocephalus* zone is end-Guadalupian (Retallack, 2005a). Additional unpublished U-Pb dates from the middle Beaufort Group also confirm such a correlation (Bruce Rubidge, 2005, personal commun.), but are at variance with the geophysically unconstrained correlations of Lucas (2005).

END-GUADALUPIAN EVENTS IN VICTORIA LAND, ANTARCTICA

The stratigraphic level on Portal Mountain that proved to contain a marked negative carbon isotope anomaly (Fig. 3) attracted our attention from the outset because of its sedimentological similarities with the Permian-Triassic boundary (Retallack et al., 2005). In addition to recording a carbon cycle crisis, Portal Mountain also preserves evidence of associated end-Guadalupian paleoenvironmental changes in paleosols and paleochannels. This part of Antarctica was a high-latitude backarc wetland during the Permian (Retallack and Krull, 1999).

Antarctic Sedimentology

A prominent sandstone bluff (Figs. 4B and 5A) in the middle Weller Coal Measures on Portal Mountain (Fig. 4A) is directly above the end-Guadalupian carbon isotope excursion (Fig. 3). This sandstone is remarkably similar to the Feather Conglomerate directly above the end-Permian carbon isotope excursion in the same section. Both conglomeratic sandstones crop out strongly and are laterally extensive marker beds. The distinctive sandstone in the Weller Coal Measures has been traced through much of Victoria Land, from Alligator Peak north to Portal Mountain, Mount Metschel, and the Fry Glacier (as "sheet sandstone lithofacies" of Isbell and Cuneo, 1996). These quartz-rich, multistory sandstones have few clayey or coaly interbeds. Trough cross-bedding is common, as are large planar foresets, which reveal less-dispersed paleocurrent directions than for other sandstones higher and lower in the sequence (Isbell and Cuneo, 1996). Broad and shallow scour and fill structures are common (Fig. 5A), but in neither unit have we been able to find steep cutbanks or low-angle lateral accretion surfaces like those in the overlying or underlying Weller Coal Measures or Buckley

the underlying Ecca Group includes *Palaeovittaria* and *Gangamopteris*, and the overlying *Dicynodon* zone (Estcourt Formation in Natal) has yielded Late Permian glossopterid fructifications, including *Rigbya, Plumsteadia*, and *Lidgettonia* (Anderson and Anderson, 1985; Gastaldo et al., 2005). The basal Katberg Formation in South Africa has yielded fragmentary

seeds, pinnules, and needles (Retallack et al., 2003; Gastaldo et al., 2005), comparable with the flora of *Lepidopteris callipteroides* and *Voltziopsis africana* from earliest Triassic rocks of Madagascar and Australia (Retallack, 2002). These megafloral changes are comparable with the Antarctic record (Fig. 3). Paleomagnetic stratigraphy confirms that the upper

TABLE 1. END-GUADALUPIAN CARBON ISOTOPE EXCURSIONS

Locality	Reference	Material analyzed	End-Guadalupian $\delta^{13}C$ excursion	End-Permian $\delta^{13}C$ excursion
Abadeh, Iran	Heydari et al., 2000	Marine limestone	−3.7	−5.1
Abadeh, Iran	Heydari et al., 2000	Marine kerogen	−1.3	−3.2
Beaufort West, South Africa	Thackeray et al., 1990	Therapsid tusks	−10.0	No data
Beaufort West, South Africa	Keith, 1969; Thackeray et al., 1990	Soil carbonate	−4.0	No data
Delaware Basin, Texas	Magaritz et al., 1983	Marine kerogen	−2.9	No data
Eddystone, Australia	Morante, 1996	Nonmarine kerogen	−3.2	−3.2
Emarat, Iran	Baud et al., 1989	Marine limestone	−1.9	−4.9
Fishburn-1, Australia	Morante, 1996	Marine kerogen	−5.1	−8
Graphite Peak, Antarctica	Krull and Retallack, 2000	Nonmarine kerogen	−16	−22.2
Idrijca, Slovenia	Dolenec and Ramovš, 1996	Marine limestone	−1.6	−2.6
Jameson Land, Greenland	Magaritz and Stemmerik, 1989	Marine limestone	−1.4	No data
Kaki Vigla, Greece	Baud et al., 1989	Marine limestone	−5.6	−2.5
Kamura, Japan	Musashi et al., 2001	Marine limestone	−1.3	−2.3
Kamura, Japan	Musashi et al., 2001	Marine kerogen	−1.8	−2.2
Morondava, Madagascar	Ghosh et al., 1998; de Wit et al., 2002	Nonmarine kerogen	−2.8	−7.9
Muswellbrook, Australia	Compston, 1960	Nonmarine kerogen	−2.2	No data
Nammal Gorge, Pakistan	Baud et al., 1996	Marine limestone	−1.7	−4.4
Paradise 1-6, Australia	Morante, 1996	Marine kerogen	−2.5	−9.4
Penglaitan, China	Wang et al., 2004	Marine limestone	−2.4	No data
Portal Mountain, Antarctica	Herein	Nonmarine kerogen	−3.4	−3.0
Raniganj Coalfield, India	de Wit et al., 2002	Nonmarine kerogen	−3.1	−13.8
Seaham Harbour, England	Magaritz and Turner, 1982	Marine limestone	−1.5	No data
Sovetashan, Armenia	Baud et al., 1989	Marine limestone	−4.5	−3.5
Talcher Coalfield, India	Ghosh et al., 1998; de Wit et al., 2002	Nonmarine kerogen	1.4	−8.8
Tieqaio, China	Wang et al., 2004	Marine limestone	−3.8	No data
Vedi, Armenia	Baud et al., 1989	Marine limestone	−3.8	−2
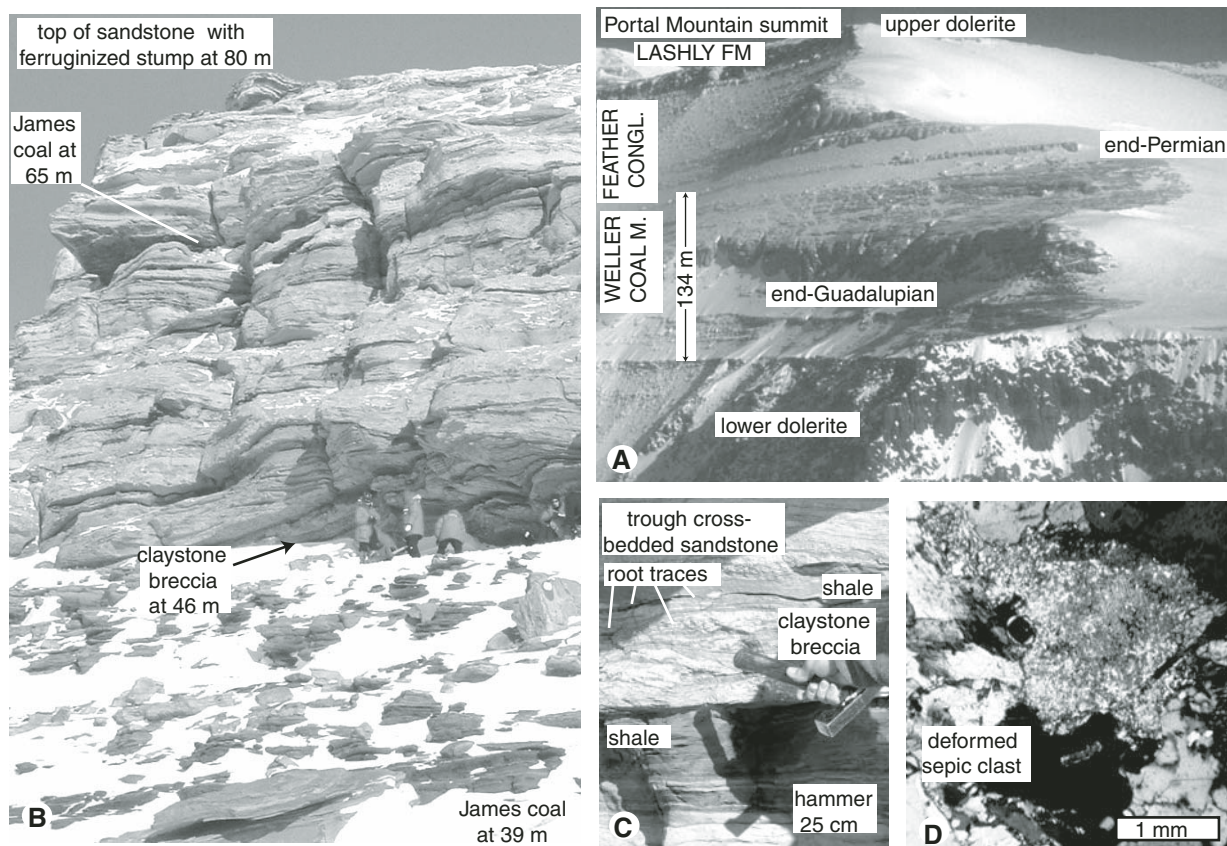
Figure 4. Portal Mountain, Antarctica, and end-Guadalupian claystone breccia. (A) The eastern ridge, here viewed from the air to the east, exposes both the end-Permian and end-Guadalupian boundaries overlain by massive sandstone. (B–C) End-Guadalupian claystone breccia in the field and in petrographic thin section viewed under crossed nicols.

Formation. Paleosols within the upper parts of fining-upward cycles within the sandstones are very weakly developed (Fig. 3), unlike the thick coals and other moderately developed paleosols of the overlying Weller Coal Measures and Buckley Formation (Retallack and Krull, 1999). We follow Isbell and Cuneo (1996) and Barrett and Fitzgerald (1986) in interpreting these marker sandstones of the middle Weller Coal Measures and lower Feather Conglomerate as vertically accreted in-channel bars deposited in low-sinuosity braided streams, in contrast with deposits of more highly sinuous streams in the upper and lower Weller Coal Measures and Buckley Formation ("tabular sandstone lithofacies" of Isbell and Cuneo, 1996; Retallack and Krull, 1999). The Feather Conglomerate is one of several earliest Triassic deposits considered to be evidence for widespread stream destabilization following end-Permian plant extinctions (Retallack, 1999; Ward et al., 2000). A similar scenario may explain the switch from high- to low-sinuosity rivers following end-Guadalupian extinctions, then return to high-sinuosity rivers at Portal Mountain.

Claystone breccias of soil clods with distinctive sepic (streaky high-birefringence clay)

A. PORTAL MOUNTAIN, ANTARCTICA

B. KAROO NATIONAL PARK, SOUTH AFRICA

ripple cross-lamination
climbing ripple lamination
structureless
mudstone flakes
trough cross-bedding
conglomerate
horizontal lamination
mudrock
fossil leaves
fossil wood
fossil bone

Figure 5. Field sketches and sedimentological sections of post-Guadalupian sandstones interpreted as deposits of braided streams at Portal Mountain Antarctica (A: 78.10784°S, 159.29979°E) and Bulkraal, South Africa (B: 32.288889°S, 22.565556°E).

microscopic fabric known from Permian-Triassic boundary sites (Retallack, 2005b) are also found at the end-Guadalupian stratigraphic level immediately beneath and below the channel sandstone on Portal Mountain (Figs. 4C and 4D). Sepic soil clods are highly water soluble, as is apparent in thin sections from Portal Mountain, where clods are deformed and expanded into grain interstices (Fig. 4C). In contrast with widespread and scattered gray mudstone flakes, which are argillasepic in thin section (Fig. 5), claystone breccia beds have pink to white equant clasts that are mosepic in thin section. The claystone breccia beds are not considered channel lags because some are isolated lenses within shale. The claystone breccia at the base of the massive sandstone is capped by shale and contains root traces, indicating that it was a depositional event separate from the overlying sandstone (Fig. 4C). As in modern forestry clearings in Oregon, these claystone breccias are interpreted as an episode of soil erosion and debris flows, possibly as a result of a rapid dieback of floodplain vegetation (Retallack, 2005b).

Antarctic Paleopedology

Unlike the Permian-Triassic boundary in Antarctica, which is a marked break in ecosystems as represented by their paleosols (Retallack et al., 2005), the end-Guadalupian life crisis was not a profound change in soils. Coaly paleosols (James pedotype) are rare within and immediately above the prominent marker sandstone but common below the sandstone (Fig. 3). The most common paleosols across the end-Guadalupian transition on Portal Mountain are Douglas pedotype (Figs. 3 and 6A–6B), here named for Sir Douglas Mawson, a pioneering Australian-Antarctic geologist. Douglas paleosols are silty and sandy, with disrupted but clear relict bedding and ellipsoidal siderite nodules at shallow depths within the profiles (Fig. 6A). Some of these siderite nodules have marginal synersis cracks and are eroded by frost and salt into a distinctive starburst pattern (Fig. 6B). Root traces in Douglas paleosols are slender with orthogonal laterals, and associated stem impressions also suggest that vegetation of these immature sandy soils was largely composed of equisetaleans (comparable horsetails and root traces are illustrated by Mader, 1990). Modern soilscapes comparable with end-Guadalupian and post-Guadalupian paleosol assemblages were discussed by Retallack (1999), and are found around Cumberland Lake, Saskatchewan (map unit Od-1a of Food and Agriculture Organization, 1975) near peat-bogs (muskeg) and lakes, respectively.

Like comparable sideritic Early Triassic Avalon and Wybung pedotypes of Australia (Retallack, 1997a, 1999), Douglas paleosols are probably Aquents in the U.S. taxonomy (Soil Survey Staff, 2000). Avalon, Wybung, and Douglas pedotypes present a geochemical conundrum of chemically reduced siderite in close proximity within a sandy soil with burrows and root traces requiring oxidation. These sandy paleosols are distinct from coaly and carbonaceous paleosols (Histosols) with siderite nodules, which have common modern analogs (Moore et al., 1992). The siderite nodules are not later diagenetic features, because some were avoided by burrows of insects, thus indicating a redoxocline in these sandy sideritic soils much steeper than at present (Retallack, 1997a). The earliest Triassic redoxocline in lowland soils was especially steep in Antarctica, judging from Dolores paleosols, which have pedogenic nodules of the oxygen-intolerant mineral berthierine (Sheldon and Retallack, 2002). Lowland soil stagnation of the earliest Triassic may have extinguished swamp woodlands of *Glossopteris* (Retallack et al., 2005). Comparable soil stagnation indicated by Douglas paleosols in the middle Weller Coal Measures may have played a role in end-Guadalupian lowland plant extinctions.

Antarctic Paleobotany

Our collections of fossil plants at Portal Mountain (Figs. 3 and 7) show very different fossil plants in the middle and upper Weller Coal Measures, with the exception of long-ranging equisetalean stems (*Paracalamites australis*) and glossopterid roots (*Vertebraria australis*). Especially notable is the loss of large leaves without midribs (*Gangamopteris* and *Palaeovittaria*) and replacement of species with low-density venation (*Glossopteris formosa*, *G. damudica*) by species with high-density venation (*Glossopteris decipiens*) just below the nadir of carbon isotope values and total organic carbon (Fig. 3). Isoetalean lycopsid leaves with midrib and paired stomatal furrows (Fig. 7E) are very rare in Antarctica, yet locally common just above the carbon isotope excursion (Fig. 3). These lycopsid leaves may indicate transiently warm climatic conditions, because Paleozoic lycopsids were mainly tropical, and like modern palms, had large frost-sensitive terminal meristems (Retallack, 1997b). These paleobotanical data are sparse but compatible with significant end-Guadalupian plant extinction and paleoclimatic warming, both of which are better understood in the Karoo Basin of South Africa (Fig. 8).
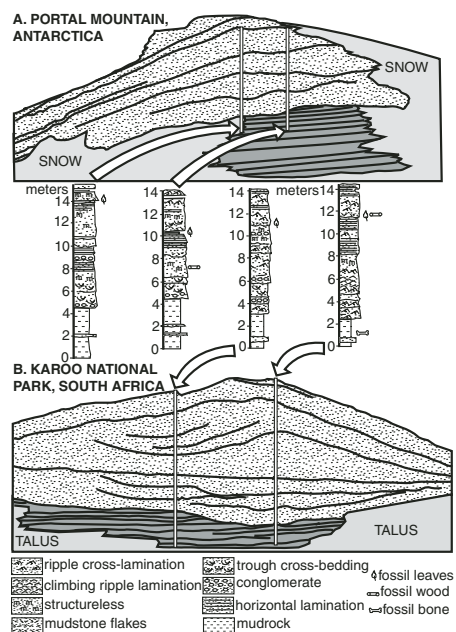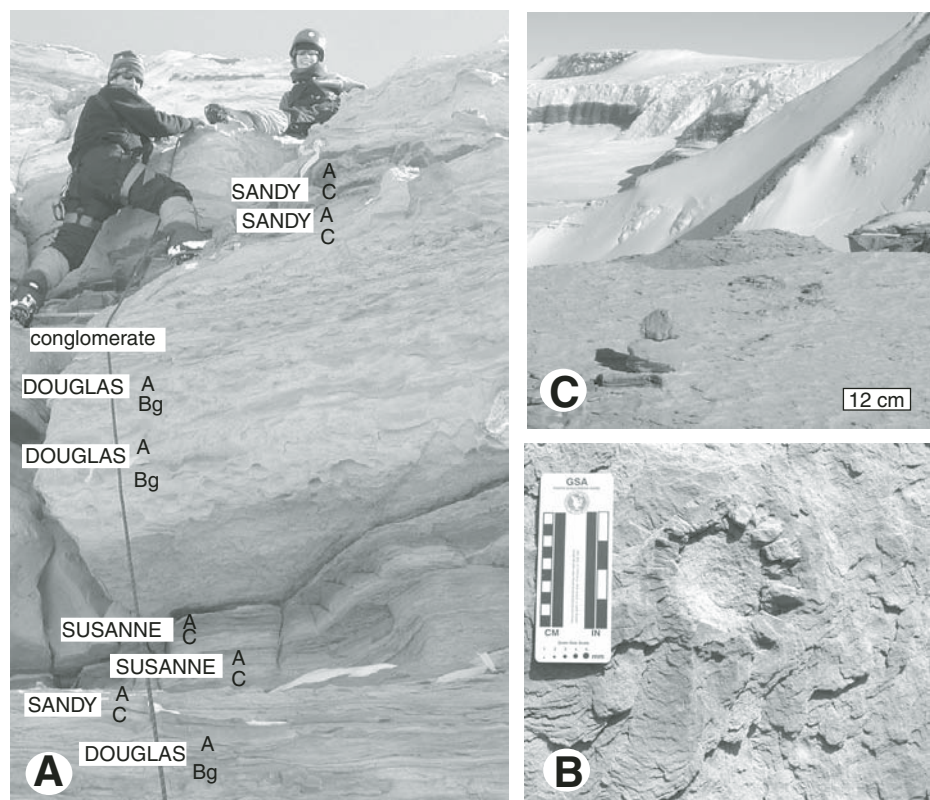
Figure 6. Permian paleosols of Portal Mountain, Antarctica: (A) Sequence of weakly developed paleosols in earliest Lopingian sandstones (50–60 m in Fig. 3). (B) Weathered siderite nodule in bedding-plane exposure of late Guadalupian Douglas pedotype (30 m in Fig. 3). (C) Silica permineralized fossil stump and log atop post-Guadalupian sandstones (80 m in Fig. 3).

END-GUADALUPIAN EVENTS IN THE KAROO BASIN, SOUTH AFRICA

The end-Guadalupian and end-Permian mass extinctions on land are especially clear in the Karoo Basin with its fossil record of vertebrates, pollen, and soils (Fig. 8). This part of Africa was a mid-latitude intracontinental arid land during the Late Permian (Retallack et al., 2003).

South African Sedimentology

As at Portal Mountain in Antarctica, both end-Guadalupian and end-Permian isotopic excursions in South Africa are associated with the appearance of thick, regionally extensive, vertically accreted, multistory sandstones, respectively, the Poortjie Sandstone Member of the Teekloof Formation and Katberg Formation (Fig. 5B). Both sandstones contain numerous stacked internal erosion surfaces lined with intraformational conglomerate up to a meter thick. These scour surfaces divide the sandstones into upward-fining depositional units that display large-scale trough cross-bedded and structureless medium-grained sandstone grading upward into ripple cross-stratified fine-grained sandstone. These widespread sandstone-dominated intervals have been interpreted as deposits of low-sinuosity rivers with highly fluctuating hydrodynamic regimes that exposed mid-channel braid bars at low stage flow (Keyser and Smith, 1979; Stear, 1980; Smith, 1995). In contrast, the predominantly single-storied sandstones of the Abrahamskraal, Upper Teekloof, and Upper Balfour Formations are characterized by fewer internal erosion surfaces that form low-angle lateral-accretion surfaces, fewer massive sandstone intervals, smaller and deeper trough cross-bedded sets, and conglomeratic lags confined to basal scour. These features have been interpreted as the deposits of point bars, scroll bars, and levees of large meandering rivers (Smith, 1990, 1993a, 1993b). In both the Poortjie and lower Katberg sandstones, weakly developed paleosols indicate accelerated rates of sediment accumulation (Retallack et al., 2003). The rapid end-Guadalupian change in fluvial style in the Karoo Basin from a few Mississippi-sized meandering channels to a network of unstable, wide, low-sinuosity channels with downstream-accreting mid-channel braid bars represented by the Poortjie sandstone may indicate landscape destabilization comparable to that thought to have followed end-Permian plant extinction (Ward et al., 2000).

South African Paleopedology

The end-Guadalupian transition in South Africa ushered in several new soil types (Fig. 9), but was not a major change of paleosols, like the end-Permian in South Africa (Retallack et al., 2003). Post-Guadalupian rocks have paleosols with carbonate nodules deeper than 40 cm below the surface: Tamka, Kanni, and Kuta pedotypes ("thick," "root," and "den," respectively in the Khoisan language: Bleek, 1956). Tamka paleosols are olive gray to bluish gray in color with stout woody root traces, and are similar to shallow calcic Bada pedotype paleosols before and after the end-Guadalupian interval. Both were probably gleyed Aridisols supporting seasonally wet woodland and desert shrubland, respectively. Kanni paleosols are weak red with common gray root haloes and other mottles, and are similar to shallow calcic Num ("purple") pedotype paleosols before and after the end-Guadalupian interval. These were probably Aridisols, supporting dry woodland and desert shrub land, respectively. Kuta paleosols of post-Guadalupian rocks were probably Alfisols, and also are found in earliest Triassic rocks (Retallack et al., 2003). Pedotypes ranging through the end-Guadalupian interval include Pawa (gray clayey Fluvents of streamside early successional vegetation), Zam (red silty Fluvents of lake-margin early successional vegetation), and Du (gray Psamments of riparian woodland).

These general indications of moderately wetter climate following the end of the Guadalupian can be quantified by comparison with the known relationship between depth to carbonate and mean annual rainfall. Modern calcareous soils have deeper carbonate nodules in wetter climates. Using a transfer function for this relationship from modern soils (Retallack, 2005c) and correcting for burial compaction of the paleosols (Sheldon and Retallack, 2001; Retallack et al., 2003) indicates that mean annual precipitation increased from ~400 mm to 800 mm at the end of both the Guadalupian and Permian in the Karoo Basin. Between transient pluvials, conditions were generally arid, as indicated by gypsum "desert roses," modest chemical weathering, and loess siltstones in the paleosols (Fig. 8C). Analogous modern soilscapes for the dry climatic times are the cold desert of Kyzl Kum and Kara Kum in Kazakhstan (map unit Yk44–3a of Food and Agriculture Organization, 1978), and for the wet climatic times, the loessic piedmont of Uzbekistan (map unit Xk 4–2b; Retallack et al., 2003).
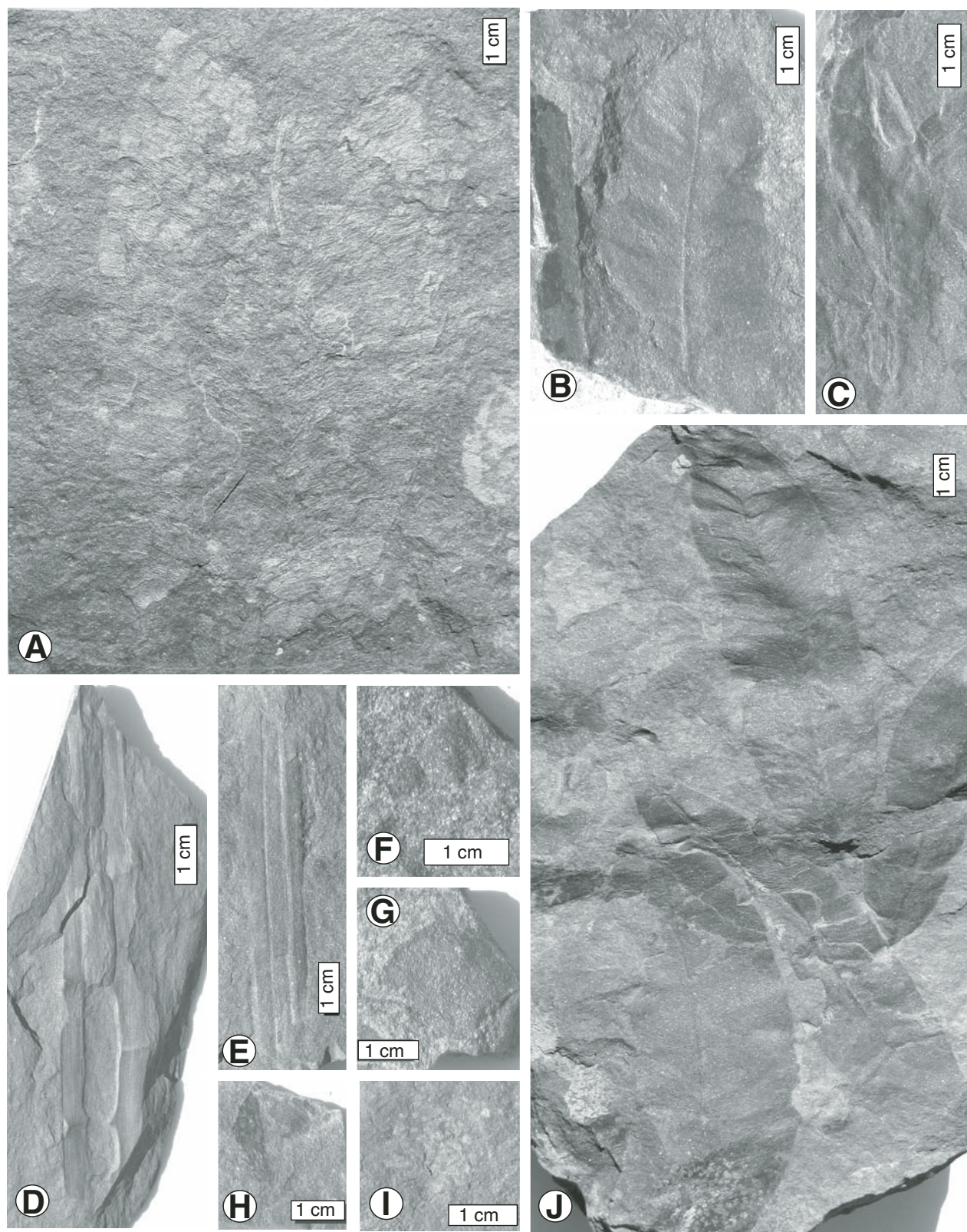
Figure 7. Fossil plants from Portal Mountain, Antarctica: (A) *Gangamopteris ovata* **(F37111) from 39 m; (B)** *Glossopteris browniana* **(F37112) from 88 m; (C)** *Glossopteris gladiforma* **(F37113) from 88 m; (D)** *Glossopteris ampla* **(below) and** *Glossopteris bucklandensis* **(above: F37109) from 88 m; (E)** *Vertebraria australis* **(F37114) from 40 m; (F)** *Lepidophyllum* **sp. indet. (F37115) from 40 m; (G)** *Squamella australis* **(F37116) from 88 m; (H)** *Plumsteadia* **sp. indet. (F37117) from 39 m; (I)** *Dictyopteridium walkomii* **(F37118) from 88 m; (J)** *Eretmonia* **sp. indet. (F37119) from 88 m. Specimen numbers are for the Condon Collection, University of Oregon. Scale bars are all 1 cm.**
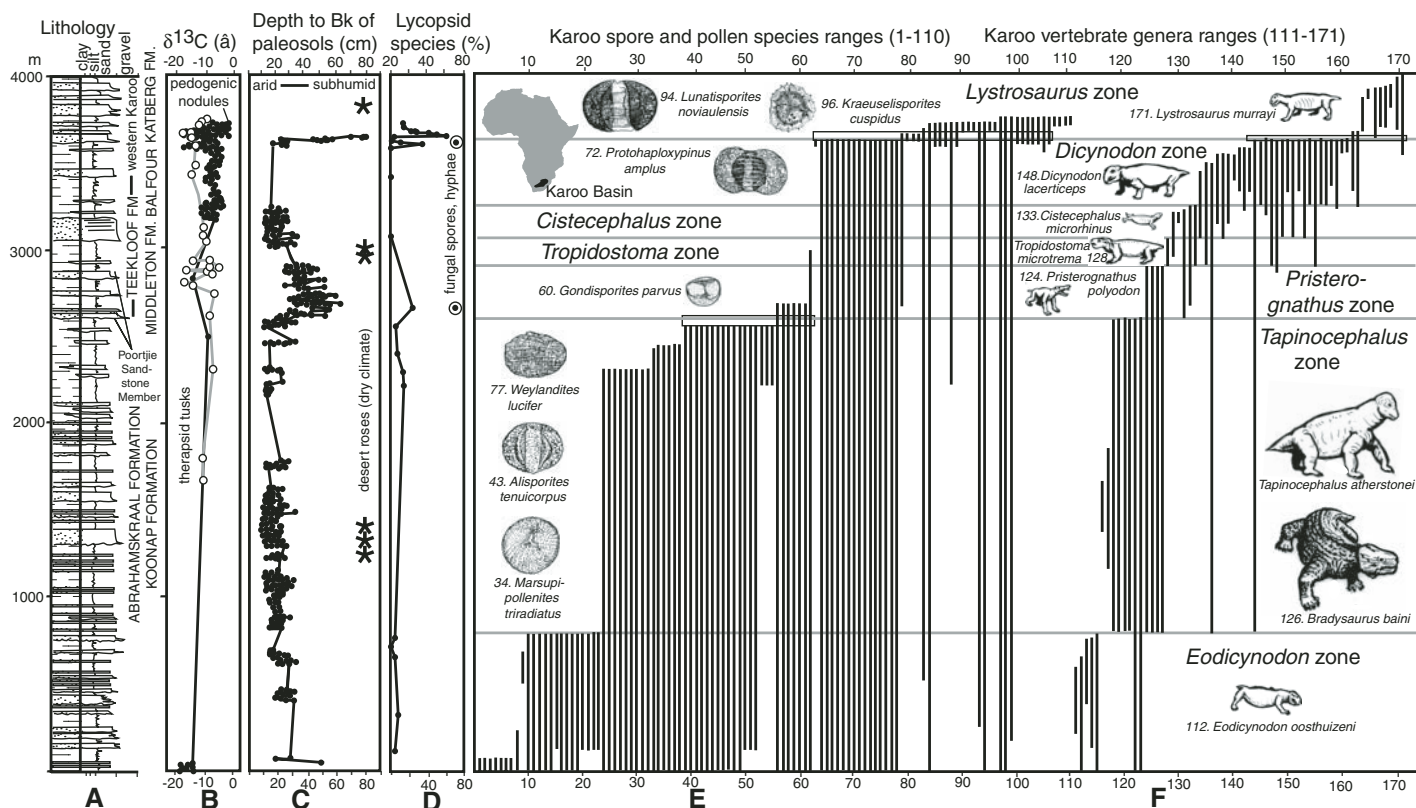
South African Palynology

Palynomorphs indicate unusual abundances of fungi and algae in South Africa after both the end of the Guadalupian and Permian (Fig. 8D). The fungi are represented by spores (Horowitz, 1990; Steiner et al., 2003), and the algae are represented by cysts (acritarchs) as well as thalli of aquatic zygnematalean algae (Krassilov et al., 1999; Foster, 2001: including "fungal hyphae" of Steiner et al., 2003). Algal spikes indicate expanded lakes or floods, supporting sedimentological and paleopedological evidence for braided streams and wet climate after the end-Guadalupian and end-Permian. Spikes in fungal spore abundance may represent unusual episodes of plant decay after mass extinction (Visscher et al., 1996).

Both end-Guadalupian and end-Permian were followed by short-term climatic warming, indicated by transient increases in diversity and abundance of lycopsid spores (Fig. 8D). Most Permian and Triassic lycopsids were tropical and had large frost-sensitive terminal meristems (Retallack, 1997b). Lycopsids expanded their range into high-latitude lowland woodlands during times of marked global warming at the end-Guadalupian and end-Permian.

These paleoclimatic excursions coincide with marked extinctions of plants in the Karoo Basin. Taken at face value, our compilation of spore and pollen ranges shows end-Guadalupian extinction of 34% of form species, and end-Permian extinction of 44% of spore pollen taxa (Fig. 8E). Recalculating extinction levels using 76 m range extension for 50% confidence interval at the end-Guadalupian, and 88 m of range extension for 50% confidence interval at the end-Permian (following methods of Marshall, 1998), gives slightly different results when short-ranging species with poorly constrained range termination are disregarded: palynospecies extinction of 30% for the end-Guadalupian and 37% for the end-Permian. By either estimate, these are significant turnovers for pollen and spores, which are common, easily recycled into younger sediments, and less affected by mass extinctions than associated animals. South African end-Guadalupian and end-Permian plant extinctions are both comparable with 30% palynological extinction at the Permian-Triassic boundary in southeastern Australia (Retallack, 1995) and 30% extinction of pollen and spores across the Cretaceous-Tertiary boundary in North Dakota (Nichols, 2002).

The end-Guadalupian extinction terminated trilete *Granulatisporites* spores and monosaccate *Florinites* pollen, which, judging from their known affinities (Balme, 1995), represent local extinction of botryopterids and cordaites, respectively. Striate bisaccate pollen grains of swampland glossopterids, such as *Protohaploxypinus*, dominate a lower-diversity flora of the *Cistecephalus* to *Dicynodon* vertebrate zones until complete extirpation of glossopterids at the end of the Permian. The end-Guadalupian and end-Permian extinctions provide an upper and lower limit to the distinctive megafossil flora dominated by fine-meshed *Glossopteris* in the *Dicynodon* zone, Estcourt Formation of Natal (Anderson and Anderson, 1995). An earliest Triassic recovery flora produced coarsely striate bisaccate conifer pollen such as *Lunatisporites* and nonstriate bisaccate seed fern pollen such as *Alisporites* (Steiner et al., 2003).

South African Vertebrate Paleontology

Extinctions of vertebrate genera in the Karoo Basin were more profound for the end-Permian at 90% than for the end-Guadalupian at 67% (Fig. 8F). These data were interpreted by Ward et al. (2005) as the culmination of gradual Late Permian decline, but reanalysis of these data by Marshall (2005) shows that they are compatible with catastrophic end-Permian extinction. Data are not available on individual occurrences to determine probable end-Guadalupian range terminations using methods of Marshall (1998, 2005), but there are indications that end-Guadalupian extinction of 67% is conservative. The

Figure 8 (*on previous page*). **Late Permian environmental and fossil record of the Karoo Basin, South Africa. (A) Lithological log of massive sandstones following both end-Guadalupian and end-Permian (from Rubidge, 1995). (B) Negative carbon isotope anomalies from pedogenic carbonate and therapsid tusks at the end-Guadalupian and end-Permian (Keith, 1969; Faure et al., 1995; MacLeod et al., 2000; Ward et al., 2005; Thackeray et al., 1990; see also GSA Data Repository [see text footnote 1]). (C) Depth to calcareous nodules in paleosols indicating arid conditions interrupted by increased mean annual precipitation following the end-Guadalupian and end-Permian (Retallack et al., 2003; Retallack, 2005a). (D) Lycopsid spore (***Gondisporites, Densiosporites, Endosporites, Laevigatosporites, Cirratriradites***) diversity, indicating warmer climate following end-Guadalupian and end-Permian, and fungal spores, indicating enhanced decay at those times (Horowitz, 1990; Steiner et al., 2003). (E–F) Ranges of fossil pollen and spores (Anderson, 1977; Stapleton, 1978; Horowitz, 1990; Steiner et al., 2003) and of vertebrate genera (Ward et al., 2005) showing mass extinctions at the end-Guadalupian and end-Permian. Palynospecies are as follows (see Depository Item [text footnote 1] for synonymies), 1—*Granulatisporites papillosus*, 2—*Striatopodocarpites fusus*, 3—*Fimbriaesporites densus*, 4—*Circulisporites parvus*, 5—*Verrucosisporites naumovae*, 6—*Protohaploxypinus hartii*, 7—*Guttulapollenites hannonicus*, 8—*Lophotriletes novicus*, 9—*Jugasporites* sp. indet., 10—*Striomonosaccites* sp. indet., 11—*Striatopodocarpites rarus*, 12—*Spinosporites spinosus*, 13—*Punctatisporites intrareticulatus*, 14—*Striatopodocarpites cancellatus*, 15—*Protohaploxypinus globus*, 16—*Protohaploxypinus diagonalis*, 17—*Marsupipollenites striatus*, 18—*Densipollenites indicus*, 19—*Striatopollenites octostriatus*, 20—*Vittatina minima*, 21—*Apiculatisporis minutus*, 22—*Laevigatosporites colliensis*, 23—*Cycadopites nevesii*, 24—*Concavisporites mortonii*, 25—*Striatoabietites multistriatus*, 26—*Gondisporites braziliensis*, 27—*Gondisporites echinatus*, 28—*Gondisporites raniganjensis*, 29—*Gondisporites punctatus*, 30—*Microbaculispora medio-granulata*, 31—*Microbaculispora plicata*, 32—*Microbaculispora fine-granulata*, 33—*Vestigisporites rudis*, 34—*Marsupipollenites triradiatus*, 35—*Cirratriradites australensis*, 36—*Didecitriletes ericianus*, 37—*Granulatisporites trisinus*, 38—*Polypodiisporites detritus*, 39—*Granulatisporites micronodosus*, 40—*Lueckisporites nyakapendensis*, 41—*Alisporites potoniei*, 42—*Horriditriletes ramosus*, 43—*Alisporites tenuicorpus*, 44—*Lueckisporites neohannonicus*, 45—*Labiisporites nectus*, 46—*Praecolpatites sinuosis*, 47—*Lueckisporites asulcus*, 48—*Plicatipollenites gondwanensis*, 49—*Cannanoropollis janaki*, 50—*Striatopodocarpites communis*, 51—*Polypodiisporites mutabilis*, 52—*Vittatina africana*, 53—*Calamospora aplata*, 54—*Inapertisporites vesiculatus*, 55—*Partimtactosporites verrucosus*, 56—*Altitriletes densus*, 57—*Platysaccus radialis*, 58—*Microbaculispora virkkiae*, 59—*Florinites eremus*, 60—*Gondisporites parvus*, 61—*Deltiodospora directa*, 62—*Apiculatisporis cornutus*, 63—*Reticuloidosporites wardianus*, 64—*Granulatisporites microgranifer*, 65—*Acanthotriletes tereteangularis*, 66—*Apiculatosporis levis*, 67—*Calamospora plicata*, 68—*Cyclogranosporites bharadwaji*, 69—*Inapertisporites inapertus*, 70—*Laevigatisporites vulgaris*, 71—*Lueckisporites cancellatus*, 72—*Protohaploxypinus amplus*, 73—*Protohaploxypinus goraiensis*, 74—*Alisporites ovatus*, 75—*Vestigisporites balmei*, 76—*Vittatina magma*, 77—*Weylandites lucifer*, 78—*Pteruchipollenites indarraensis*, 79—*Vittatina ovalis*, 80—*Lueckisporites singhi*, 81—*Triplexisporites playfordi*, 82—*Protohaploxypinus jacobi*, 83—*Protohaploxypinus limpidus*, 84—*Limitisporites monstruosus*, 85—*Falcisporites stabilis*, 86—*Guthoerlisporites cancellosus*, 87—*Densoisporites complicatus*, 88—*Punctatisporites gretensis*, 89—*Protohaploxypinus varius*, 90—*Laevigatosporites callosus*, 91—*Lunatisporites transversundatus*, 92—*Lundbladispora brevicula*, 93—*Lunatisporites* sp. indet., 94—*Lunatisporites noviaulensis*, 95—*Kraeuselisporites* sp. indet., 96—*Kraeuselisporites cuspidus*, 97—*Platysaccus papilionis*, 98—*Cycadopites follicularis*, 99—*Platysaccus leschicki*, 100—*Falcisporites zapfei*, 101—*Klausipollenites schaubergeri*, 102—*Protohaploxypinus microcorpus*, 103—*Strotersporites richteri*, 104—*Protohaploxypinus samoilovichii*, 105—*Lunatisporites pellucidus*, 106—*Densoisporites playfordii*, 107—*Spinotriletes senecioides*, 108—*Triadispora staplinii*, 109—*Alisporites australis*, 110—*Endosporites hexareticulatus*. Vertebrate genera (modified from Ward et al., 2005) include 111—*Patranomodon*, 112—*Eodicynodon*, 113—genus uncertain, 114—*Australosynodon*, 115—*Tapinocaninus*, 116—*Galeops*, 117—*Broomia*, 118—*Anteosaurus*, 119—*Titanosaurus*, 120—*Jonkeria*, 121—*Robertia*, 122—*Glanosuchoides*, 123—*Alopecodon*, 124—*Pristerognathus*, 125—*Eunotosaurus*, 126—*Bradysaurus*, 127—*Embrithosaurus*, 128—*Tropidostoma*, 129—*Rhachiocephalus*, 130—*Platycyclops*, 131—*Gorgonops*, 132—*Endothiodon*, 133—*Cistecephalus*, 134—*Aulacocephalodon*, 135—*Pareiasaurus*, 136—*Pristerodon*, 137—*Dinanomodon*, 138—*Clelandia*, 139—*Dinogorgon*, 140—*Spondylolestes*, 141—*Anthodon*, 142—*Millerosaurus*, 143—*Millereta*, 144—*Diictodon*, 145—*Emydops*, 146—*Oudenodon*, 147—*Pelanomodon*, 148—*Dicynodon*, 149—*Lycaenops*, 150—*Cynosaurus*, 151—*Prorubidgea*, 152—*Leontocephalus*, 153—*Rubidgea*, 154—*Broomicephalus*, 155—*Ictidosuchoides*, 156—*Theriognathus*, 157—*Homodontosaurus*, 158—*Promoschorhynchus*, 159—*Procynosuchus*, 160—*Cynosaurus*, 161—*Nanictosaurus*, 162—*Tratracynodon*, 163—*Moscorhinus*, 164—*Proterosuchus*, 165—*Oliveria*, 166—*Scaloposaurus*, 167—*Thrinaxodon*, 168—*Galesaurus*, 169—*Myosaurus*, 170—*Procolophon*, 171—*Lystrosaurus*.**

data of Ward et al. (2005) used here, include only 12 taxa in the *Tapinocephalus* zone, whereas Rubidge (1995) lists 46 taxa of fish, amphibians, and reptiles, many with very uncertain ranges.

The principal casualties of the end-Guadalupian extinction were all 18 South African genera of Dinocephalia, excluding *Tapinocephalus*, which is less common than is ideal for a zonal index fossil and does not range to the end of the zone. Principal casualties of the end-Permian extinction include all Gorgonopsian and Biarmosuchian predators, and most Dicynodontian herbivores, with the exception of *Lystrosaurus*. Large body size (~100 kg) is impressive in *Bradysaurus* and *Dicynodon*, but immediately after

both the end-Guadalupian and end-Permian extinctions, survivors were small (20–50 kg) and commonly found in burrows (Retallack et al., 2003). Vertebrate burrow casts are common in the postapocalyptic greenhouse following both the end-Guadalupian crisis (Smith, 1987), when they were excavated by *Diictodon*, and end-Permian crisis (Retallack et al., 2003), when excavated by *Lystrosaurus* (Groenewald, 1991).

LATE PERMIAN EXTINCTIONS RECONSIDERED

End-Guadalupian extinction of marine invertebrates was comparable in magnitude

with the end-Cretaceous mass extinction (Stanley and Yang, 1994). Similarly, end-Guadalupian extinctions of plants and animals on land in the Karoo Basin are comparable in magnitude with end-Cretaceous extinction of plants and animals in Montana, USA (Nichols, 2002; Fastovsky and Sheehan, 2005). The end-Guadalupian mass extinction was a major event in its own right, both on land and at sea. Mechanisms of Permian mass extinction on land can now be reconsidered as two geologically abrupt mass extinctions separated by stable conditions, rather than a gradual Late Permian decline (Benton et al., 2004; Ward et al., 2005).
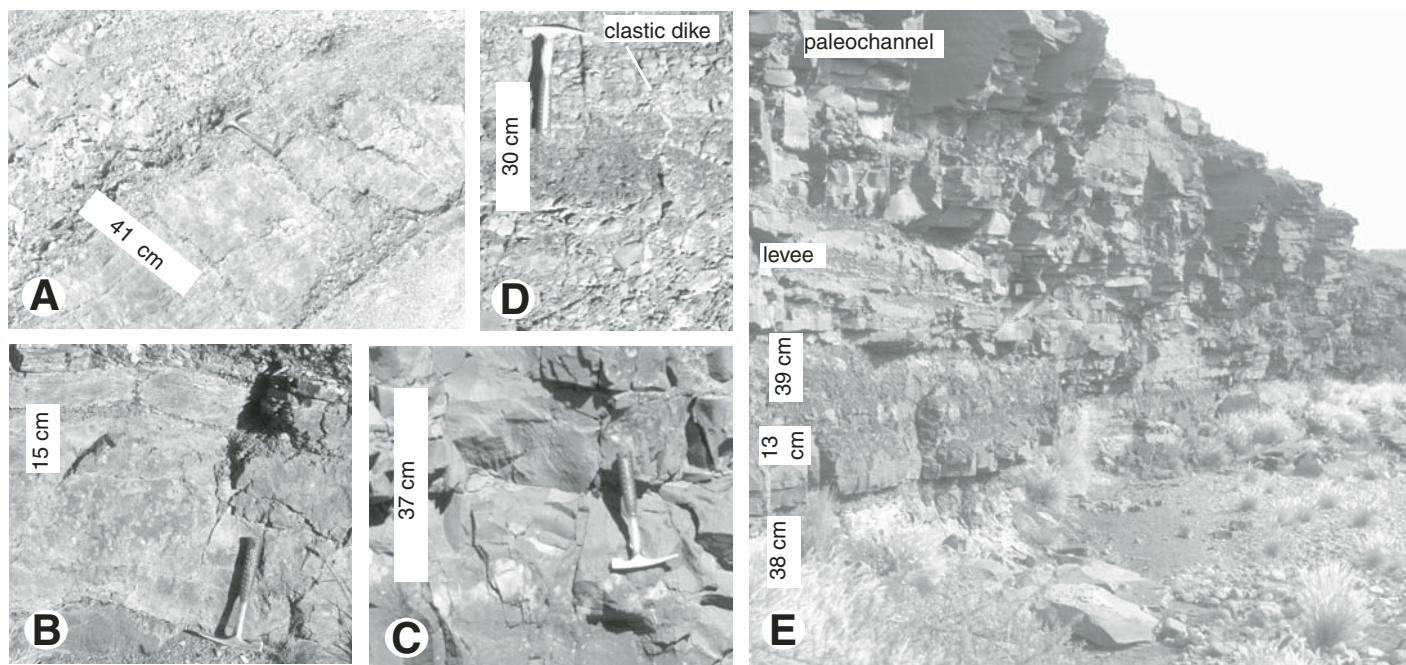
Figure 9. Middle-Late Permian paleosols of the Karoo Basin, showing measured distance between top (below bedded overburden) and Bk horizon (white calcareous nodules). (A) Type Tamka pedotype, *Eodicynodon* zone, north-dipping Abrahamskraal Formation (980 m above base), 2 km north of Modderdrift (33.076833°S, 22.533583°E). (B) Bada pedotype, *Tapinocephalus* zone, Abrahamskraal Formation (1028 m above base), 5 km north of Modderdrift (33.053183°S, 22.535617°E). (C) Tamka pedotype, *Pristerognathus* zone, Poortjie Sandstone Member, Teekloof Formation (133 m above base), near Amandelhoogte Farm (33.787317°S, 22.57896°E), 47 km south of Beaufort West. (D) Som pedotype, *Cistecephalus* zone, Hoedemaker Member, Teekloof Formation (282 m above base), above first switchback in highway, Teekloof Pass (32.2031°, 22.616783°E). (E) Som (below) and Zam pedotypes (in paleolevee), *Pristerognathus* zone, Hoedemaker Member, Teekloof Formation (290 m above base), Gamka River 3 km east of Karoo National Park Headquarters (32.2961°S, 22.562883°E). For further details see Depository Item of Retallack et al. (2003).

The end-Permian extinction is no longer a unique event, because it shares with the end-Guadalupian extinction a postapocalyptic warm-wet greenhouse, a spike of lycopsids, fungi, and algae, marked soil erosion and soil stagnation, and dominance of braided streams (Fig. 10). Both carbon cycle crises were global, as indicated by 17 sites worldwide for the end-Guadalupian isotopic excursion, and 55 sites for the end-Permian isotopic excursion (Fig. 2). Stomatal index of seed ferns in sites from northern Russia to southeastern Australia also indicates that these were global events of high atmospheric CO_2 (Retallack, 2002, 2005a). These transient greenhouse warming events were particularly striking at high paleolatitudes. In Arctic Canada, glacial dropstones are found in Middle to Late Permian marine sandstones, but the end-Guadalupian warm spike is represented by a marine transgression of bryozoan-rich Degeböls Limestone within noncalcareous sandstones (Beauchamp and Thériault, 1994). In southeastern Australian sequences with Middle Permian periglacial paleosols, marine glendonites, and glacial dropstones, the end-Guadalupian warm spike is represented by a marine transgression of calcareous Kulnura Marine Tongue within the noncalcareous Tomago Coal Measures, and by kaolinitic paleosols (Ultisols) of the Dunedoo Formation (Retallack, 2005a).

Both end-Guadalupian and end-Permian carbon isotopic excursions were drops of at least $-4‰$ $\delta^{13}C_{org}$, which mass balance calculations (Berner, 2002) demonstrate to be feasible only with release to the atmosphere of large amounts (~2000 Gt) of methane of very isotopically depleted composition ($\delta^{13}C$ ~$-60‰$). Such models (Berner, 2002, 2005) also reveal that a combination of methane oxidation, together with ongoing contributions from decay and volcanism may have reduced earliest Triassic atmospheric oxygen to some 15%, much lower than current (21%) or modeled earlier Permian levels (30%). With their coarse temporal resolution of 10 m.y. increments (Berner, 2002, 2005; Bergman et al., 2004), these models conflate the end-Guadalupian and end-Permian atmospheric crises. These were distinct crises separated by 9 m.y., as indicated by carbon isotope and paleosol evidence presented here, as well as from stomatal index studies of seed ferns (Retallack, 2002).

Both end-Guadalupian and end-Permian mechanisms of extinction may have been similar. Oxygen shortage and high carbon dioxide levels were critical for marine corals and brachiopods, with passive ventilation for respiration, but less serious for clams and ammonoids with active ventilation (Knoll et al., 1996). Oxygen shortage was also critical to root respiration of plants in lowland swampy habitats where paleosols reveal chemically reducing conditions (Sheldon and Retallack, 2002; Sheldon, 2006). Deforestation of stagnant soils thus resulted in claystone breccias (Retallack, 2005b) and braided streams (Ward et al., 2000). For land animals, earliest Triassic oxygen levels may have been equivalent to those now found at high elevations where there is elevated risk of death by pulmonary edema (Huey and Ward, 2005). Small, burrowing animals that had adapted to low oxygen conditions survived preferentially. Other evolutionary advances promoted by successive Late Permian atmospheric crises were development of the bony secondary palate, creation of an unobstructed airway, and reduction of thoracic ribs, perhaps due to development of a muscular diaphragm
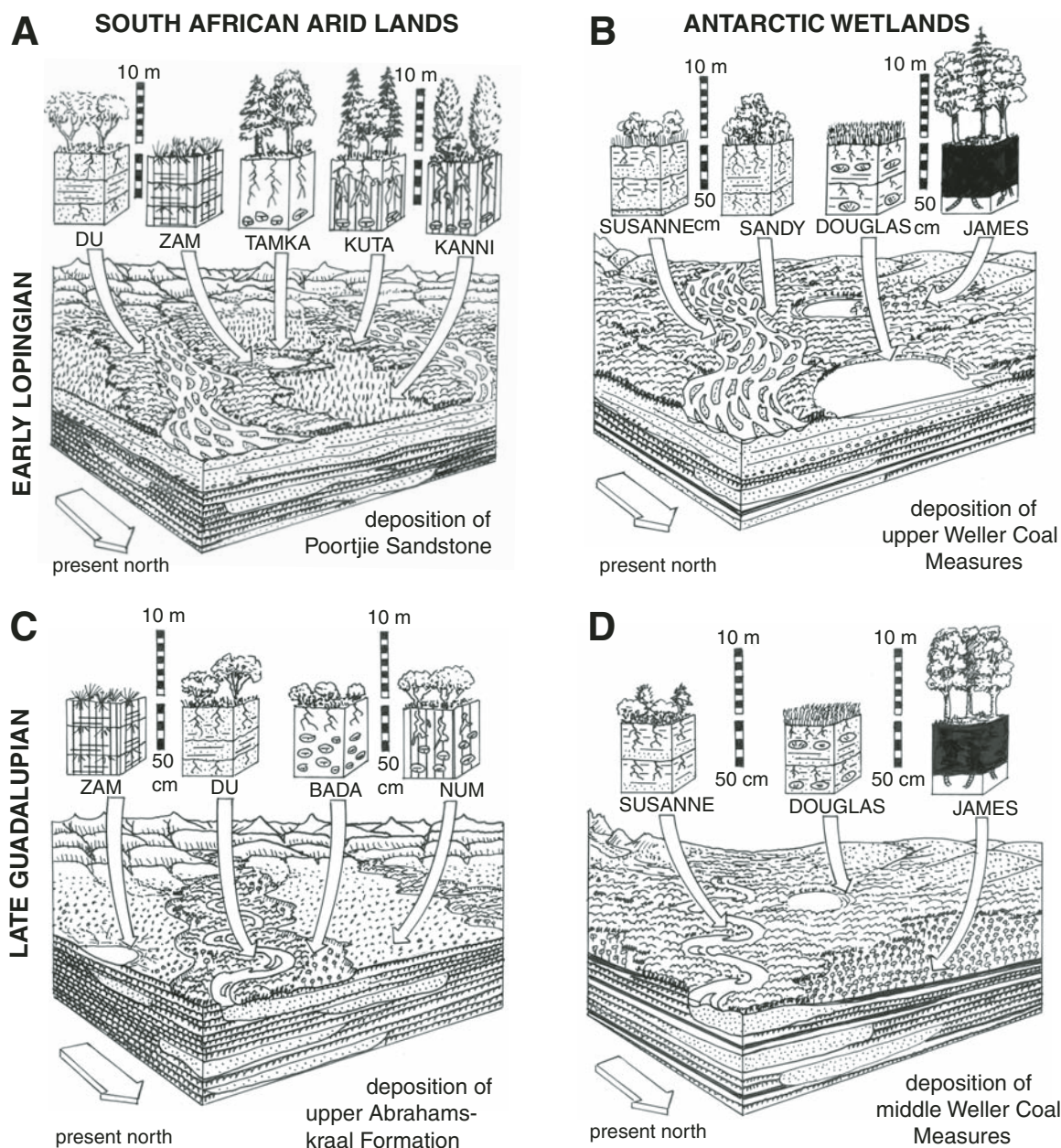
Figure 10. Ecosystem shift before (A–B) and after (C–D) end-Guadalupian life crisis in high-latitude arid lands of South Africa (A, C) and polar wetlands of Antarctica (B, D).

(Retallack et al., 2003). Late Permian atmospheric crises may have been important selective pressures in the evolution of mammalian anatomical and physiological adaptations.

A significant problem remaining with this scenario is how the necessarily large amounts (10^2–10^3 Gt) of methane were released into the atmosphere on short time scales (10^4–10^5 yr). Asteroid impact into a marine or permafrost reservoir of methane clathrate is one possibility, but the end-Permian "Bedout Crater" (Becker et al., 2004) remains controversial

(Wignall et al., 2004), and we are unaware of a suitable end-Guadalupian crater. Submarine landslide of clathrate reservoirs also is plausible and known for the end-Permian but not the end-Guadalupian (Retallack et al., 2005). A more promising source of methane is mobilization of coal-bed methane by igneous intrusion (McElwain et al., 2005), because both the end-Guadalupian Emeishan traps (Zhou et al., 2002) and end-Permian Siberian traps (Kamo et al., 2003) erupted through pre-existing coal measures. Although degassing of flood basalt

lavas is insufficient to explain observed extinctions and atmospheric crises (Berner, 2002), their reaction with intruded coals or clathrates makes flood basalts a significant threat to planetary habitability.

REFERENCES CITED

Anderson, J.M., 1977, The biostratigraphy of the Permian and Triassic: Memoirs of the Botanical Survey of South Africa, v. 41, p. 1–67.

Anderson, J.M., and Anderson, H.M., 1985, Palaeoflora of Southern Africa: Prodromus of South African Megafloras Devonian to Lower Cretaceous: Rotterdam, A.A. Balkema, 423 p.

Balme, B.E., 1995, Fossil in situ spores and pollen grains: An annotated catalogue: Review of Palaeobotany and Palynology, v. 87, p. 81–322, doi: 10.1016/0034-6667(95)93235-X.

Bangert, B., Stollhofen, H., Lorenz, V., and Armstrong, R., 1999, The geochronology of ash-fall tuffs in the glacigenic Carboniferous-Permian Dwyka Group of Namibia and South Africa: Journal of African Earth Sciences, v. 29, p. 33–49, doi: 10.1016/S0899-5362(99)00078-0.

Barrett, P.J., and Fitzgerald, P.G., 1986, Deposition of the lower Feather Conglomerate, a Permian braided river deposit in southern Victoria Land, Antarctica, with notes on paleogeography: Sedimentary Geology, v. 45, p. 199–208.

Baud, A., Magaritz, M., and Holser, W.T., 1989, Permian-Triassic of the Tethys: Carbon isotope studies: Geologische Rundschau, v. 78, p. 649–677, doi: 10.1007/BF01776196.

Baud, A., Atudorei, V., and Sharp, Z., 1996, Late Permian and Early Triassic evolution of the northern Indian margin: Carbon isotope and sequence stratigraphy: Geodinamica Acta, v. 9, p. 57–77.

Beauchamp, B., and Thériault, O., 1994, Late Paleozoic syn- and post-rift sequences on Grinnell Peninsula, Canadian Arctic (Sverdrup basin): Evidence for basin margin tectonic disturbances associated with sequence boundaries, *in* Embry, A.F., Beauchamp, B., and Glass, D.J., eds., Pangea: Global Environments and Resources: Canadian Society of Petroleum Geologists Memoir 17, p. 199–217.

Becker, L., Poreda, R.J., Basu, A.R., Pope, K.O., Harrison, T.M., Nicholson, C., and Iasky, R., 2004, Bedout; a possible end-Permian impact crater offshore of northwestern Australia: Science, v. 304, p. 1469–1476, doi: 10.1126/science.1093925.

Benton, M.J., Tverdokhlebov, V.P., and Sukhov, M.V., 2004, Ecosystem remodelling among vertebrates at the Permian-Triassic boundary in Russia: Nature, v. 432, p. 97–100, doi: 10.1038/nature02590.

Bergman, N.M., Lenton, T.M., and Watson, A.J., 2004, COPSE: A new model of biogeochemical cycling over Phanerozoic time: American Journal of Science, v. 304, p. 397–437, doi: 10.2475/ajs.304.5.397.

Berner, R.A., 2002, Examination of hypotheses for the Permian-Triassic boundary extinction by carbon cycle modeling: U.S. National Academy of Science Proceedings, v. 99, p. 4172–4177, doi: 10.1073/pnas.032095199.

Berner, R.A., 2005, The carbon and sulfur cycles and atmospheric oxygen from middle Permian to Middle Triassic: Geochimica et Cosmochimica Acta, v. 69, p. 3211–3217, doi: 10.1016/j.gca.2005.03.021.

Bleek, D.F., 1956, A Bushman Dictionary: New Haven, Connecticut, Oriental Society, 773 p.

Chandra, S., and Singh, J.K., 1996, Plant fossils from the type locality of Talchir Formation and evidence of earliest plant/animal activity in Gondwana of India, *in* Tiku, ed., Gondwana Nine, Volume 1: Rotterdam, A.A. Balkema, p. 397–414.

Collinson, J.W., Hammer, W.R., Askin, R.A., and Elliot, D.H., 2006, Permian-Triassic boundary in the central Transantarctic Mountains, Antarctica: Geological Society of America Bulletin, v. 118, p. 747–763, doi: 10.1130/B25739.1.

Compston, W., 1960, The carbon isotope composition of certain marine invertebrates and coals from the Australian Permian: Geochimica et Cosmochimica Acta, v. 18, p. 1–22, doi: 10.1016/0016-7037(60)90013-2.

de Wit, M.J., Ghosh, J.G., de Villiers, S., Rakotosolofo, N., Alexander, J., Tripathi, A., and Looy, C., 2002, Multiple organic carbon isotope reversals across the Permo-Triassic boundary of terrestrial Gondwanan sequences: Clues to extinction patterns and delayed ecosystem

recovery: The Journal of Geology, v. 110, p. 227–240, doi: 10.1086/338411.

Dolenec, T., and Ramovš, A., 1996, Carbon and oxygen isotope variations in the Permian-Triassic boundary carbonate sequence from Idrijca Valley (W. Slovenia): Permophiles, v. 29, p. 42–44.

Falcon, R.M.S., 1975a, Palynostratigraphy of the Lower Karoo sequence in the central Sebungwe District, mid-Zambezi Basin: Rhodesia: Palaeontologia Africana, v. 18, p. 1–29.

Falcon, R.M.S., 1975b, Application of palynology in subdividing the coal-bearing formations of the Karoo sequence in southern Africa: South African Journal of Science, v. 71, p. 336–344.

Fastovsky, D.E., and Sheehan, P.M., 2005, The extinction of dinosaurs in North America: GSA Today, v. 15, no. 3, p. 4–10.

Faure, K., Harris, C., and Willis, J.P., 1995, A profound meteoric water influence on carbonate genesis in the Permian Waterberg Coalfield, South Africa; evidence from stable isotopes: Journal of Sedimentary Research, v. A65, p. 605–613.

Food and Agriculture Organization, 1975, Soil Map of the World. Volume II, North America: Paris, United Nations Educational, Scientific and Cultural Organization, 210 p.

Food and Agriculture Organization, 1978, Soil Map of the world. Volume VIII, North and Central Asia: Paris, United Nations Educational, Scientific and Cultural Organization, 221 p.

Foster, C.B., 2001, Micro-organism uncertainty casts doubt on extinction theory: Australian Geologist News, v. 61, p. 8–9.

Gastaldo, R.A., Adendorff, R., Bamford, M., Labandeira, C.C., Neveling, J., and Simms, H., 2005, Taphonomic trends of macrofloral assemblages across the Permian-Triassic boundary, Karoo Basin, South Africa: Palaios, v. 20, p. 479–497, doi: 10.2110/palo.2004.P04-62.

Ghosh, J.G., Tripathy, A., Rakotosolofo, N.A., and de Wit, M., 1998, Organic carbon isotope variation of plant remains: Chemostratigraphical markers in terrestrial Gondwanan sequences: Journal of African Earth Sciences, v. 27, p. 83–85.

Gradstein, F.M., Ogg, J.G., and Smith, A.G., 2005, A Geologic Time Scale 2004: Cambridge, Cambridge University Press, 589 p.

Groenewald, G.E., 1991, Burrow casts from the *Lystrosaurus-Procolophon* assemblage zones, Karoo sequence, South Africa: Koedoe, v. 34, p. 13–22.

Heydari, E., Hassandzadeh, J., and Wade, W.J., 2000, Geochemistry of central Tethyan Upper Permian and Lower Triassic strata, Abadeh region, Iran: Sedimentary Geology, v. 137, p. 85–99, doi: 10.1016/S0037-0738(00)00138-X.

Horowitz, A., 1990, Palynology and paleoenvironment of uranium deposits in the Permian Beaufort Group, South Africa: Ore Geology Reviews, v. 5, p. 537–540, doi: 10.1016/0169-1368(90)90052-O.

Huey, R.B., and Ward, P.D., 2005, Hypoxia, global warming and terrestrial Late Permian extinctions: Science, v. 308, p. 398–401, doi: 10.1126/science.1108019.

Isbell, J.L., and Cuneo, N.R., 1996, Depositional framework of Permian coal-bearing strata, southern Victoria Land, Antarctica: Palaeogeography, Palaeoclimatology, Palaeoecology, v. 125, p. 217–238, doi: 10.1016/S0031-0182(96)00032-6.

Isbell, J.L., Askin, R.A., and Retallack, G.J., 1999, Search for evidence of impact at the Permian-Triassic boundary in Antarctica and Australia: Comment and reply: Geology, v. 27, p. 859–860, doi: 10.1130/0091-7613(1999)027<0859:SFEOIA>2.3.CO;2.

Jahren, A.H., Arens, N.C., Sarmiento, G., Guerrero, J., and Amundson, R., 2001, Terrestrial record of methane hydrate dissociation in the Early Cretaceous: Geology, v. 29, p. 159–162, doi: 10.1130/0091-7613(2001)029<0159:TROMHD>2.0.CO;2.

Kamo, S.L., Czamanske, G.K., Amelin, Y., Fedorenko, V.A., Davis, D.W., and Trofimov, V.R., 2003, Rapid eruption of Siberian flood-volcanic rocks and evidence for coincidence with the Permian-Triassic boundary and mass extinction at 251 Ma: Earth and Planetary Science Letters, v. 214, p. 75–91, doi: 10.1016/S0012-821X(03)00347-9.

Keith, M.L., 1969, Isotopic composition of carbonates from the Karoo and comparisons with the Passa Dois Group of Brazil, *in* Amos, A.J., ed., Gondwana Stratigraphy: Paris, United Nations Educational, Scientific, and Cultural Organization, p. 775–778.

Keyser, A.W., and Smith, R.M.H., 1979, Vertebrate biozonation of the Beaufort Group with special reference to the western Karoo Basin: Geological Survey of South Africa Annals, v. 12, p. 1–35.

Knoll, A.H., Bambach, R.K., Canfield, D.E., and Grotzinger, J.F., 1996, Comparative Earth history and the Late Permian mass extinction: Science, v. 273, p. 452–457.

Krassilov, V.A., Afonin, S.A., and Baranova, S.S., 1999, *Tympanicysta* and the terminal Permian events: Permophiles, v. 35, p. 16–17.

Krull, E.S., and Retallack, G.J., 2000, $\delta^{13}C_{org}$ depth profiles from paleosols across the Permian-Triassic boundary: Evidence for methane release: Geological Society of America Bulletin, v. 112, p. 1459–1472, doi: 10.1130/0016-7606(2000)112<1459:CDPFPA>2.0.CO;2.

Kyle, R.A., 1977, Palynostratigraphy of the Victoria Group of South Victoria Land, Antarctica: New Zealand Journal of Geology and Geophysics, v. 20, p. 1081–1102.

Lucas, S.J., 2005, Permian tetrapod faunachrons, *in* Lucas, S.G., and Zeigler, K.E., eds., The Nonmarine Permian: New Mexico Museum of Natural History and Science Bulletin, v. 30, p. 197–201.

MacLeod, K.G., Smith, R.M.H., Koch, P.L., and Ward, P.D., 2000, Timing of mammal-like reptile extinctions across the Permian-Triassic boundary in South Africa: Geology, v. 28, p. 227–230, doi: 10.1130/0091-7613(2000)028<0227:TOMLRE>2.3.CO;2.

MacRae, C.S., 1988, Palynostratigraphic Correlation Between the Lower Karoo Sequence of the Waterberg and Pafuri Coal-Bearing Basins and the Hammanskraal Plant Macrofossil Locality, Republic of South Africa: Geological Survey of South Africa Memoir, v. 75, 217 p.

Mader, D., 1990, Paleoecology of the flora in the Bundstandstein and Keuper in the Triassic of middle Europe: Hannover, G. Fischer, 305 p.

Magaritz, M., and Stemmerik, L., 1989, Oscillation of carbon and oxygen isotope compositions of carbonate rocks between evaporative and open marine environments: Upper Permian of East Greenland: Earth and Planetary Science Letters, v. 93, p. 233–240.

Magaritz, M., and Turner, P., 1982, Carbon cycle changes of the Zechstein Sea; isotopic transition zone in the Marl Slate: Nature, v. 297, p. 389–390, doi: 10.1038/297389a0.

Magaritz, M., Anderson, R.Y., Holser, W.T., Saltzman, E.S., and Garber, J.H., 1983, Isotope shifts in the Late Permian of the Delaware Basin precisely timed by varved sediments: Earth and Planetary Science Letters, v. 66, p. 111–124, doi: 10.1016/0012-821X(83)90130-9.

Marshall, C., 1998, Determining stratigraphic ranges, *in* Donovan, S.K., and Paul, C.R.C., eds., The Adequacy of the Fossil Record: Chichester, John Wiley, p. 23–53.

Marshall, C., 2005, Technical comment on "Abrupt and gradual extinction among Late Permian land vertebrates in the Karoo Basin, South Africa": Science, v. 308, p. 1413b, doi: 10.1126/science.1110443.

McElwain, J., Wade-Murphy, J., and Hesselbo, S.P., 2005, Changes in carbon dioxide during an oceanic anoxic event linked to intrusion into Gondwana coals: Nature, v. 435, p. 479–482, doi: 10.1038/nature03618.

Moore, S.E., Ferrell, R.E., and Aharon, P., 1992, Diagenetic siderite and other ferroan carbonates in a subsiding marsh sequence: Journal of Sedimentary Petrology, v. 62, p. 357–366.

Morante, R., 1996, Permian and Early Triassic isotopic records of carbon and strontium in Australia and a scenario of events about the Permian-Triassic boundary: Historical Biology, v. 11, p. 289–310.

Musashi, M., Isozaki, Y., Koike, T., and Kreulon, R., 2001, Stable carbon isotope signature in mid-Panthalassa shallow water carbonates across the Permo-Triassic boundary: Evidence for ^{13}C depleted superocean: Earth and Planetary Science Letters, v. 191, p. 9–20, doi: 10.1016/S0012-821X(01)00398-3.

Nichols, D.J., 2002, Palynology and palynostratigraphy of the Hell Creek Formation in North Dakota; a

microfossil record of plants at the end of Cretaceous time, *in* Hartman, J.H., Johnson, K.R., and Nichols, D.J., eds., The Hell Creek Formation and the Cretaceous-Tertiary Boundary in the Northern Great Plains: An Integrated Continental Record of the End of the Cretaceous: Geological Society of America Special Paper 361, p. 393–456.

Payne, J.L., Lehrmann, D.J., Wei, J.Y., Orchard, M.J., Schrag, D.P., and Knoll, A.H., 2004, Large perturbations of the carbon cycle during recovery from the end-Permian extinction: Science, v. 305, p. 506–509, doi: 10.1126/science.1097023.

Retallack, G.J., 1980, Late Carboniferous to Middle Triassic megafossil floras from the Sydney Basin, *in* Helby, R.J., and Herbert, C., eds., A Guide to the Sydney Basin: Geological Survey of New South Wales Bulletin, v. 26, p. 385–430.

Retallack, G.J., 1995, Permian-Triassic life crisis on land: Science, v. 267, p. 77–80.

Retallack, G.J., 1997a, Palaeosols in the Upper Narrabeen Group of New South Wales as evidence of Early Triassic palaeoenvironments without exact modern analogues: Australian Journal of Earth Sciences, v. 44, p. 185–201.

Retallack, G.J., 1997b, Earliest Triassic origin of *Isoetes* and quillwort evolutionary radiation: Journal of Paleontology, v. 71, p. 500–521.

Retallack, G.J., 1999, Post-apocalyptic greenhouse paleoclimate revealed by earliest Triassic paleosols in the Sydney Basin, Australia: Geological Society of America Bulletin, v. 111, p. 52–70, doi: 10.1130/0016-7606(1999)111<0052:PGPRBE>2.3.CO;2.

Retallack, G.J., 2002, *Lepidopteris callipteroides*, an earliest Triassic seed fern of the Sydney Basin, southeastern Australia: Alcheringa, v. 26, p. 475–500.

Retallack, G.J., 2005a, Permian greenhouse crises, *in* Lucas, S.G., and Zeigler, K.E., eds., The Nonmarine Permian: New Mexico Museum of Natural History and Science Bulletin, v. 30, p. 256–269.

Retallack, G.J., 2005b, Earliest Triassic claystone breccias and soil erosion crisis: Journal of Sedimentary Research, v. 75, p. 679–695, doi: 10.2110/jsr.2005.055.

Retallack, G.J., 2005c, Pedogenic carbonate proxies for amount and seasonality of precipitation in paleosols: Geology, v. 33, p. 333–336, doi: 10.1130/G21263.1.

Retallack, G.J., and Krull, E.S., 1999, Landscape ecological shift at the Permian-Triassic boundary in Antarctica: Australian Journal of Earth Sciences, v. 46, p. 785–812, doi: 10.1046/j.1440-0952.1999.00745.x.

Retallack, G.J., and Krull, E.S., 2006, Carbon isotopic evidence for terminal-Permian methane outbursts and their role in extinctions of animals, plants, coral reefs, and peat swamps, *in* Greb, S.F., and DiMichele, W.A., eds., Wetlands Through Time: Geological Society of America Special Paper 399, p. 249–268.

Retallack, G.J., Smith, R.M.H., and Ward, P.D., 2003, Vertebrate extinction across the Permian-Triassic boundary in the Karoo Basin, South Africa: Geological Society of America Bulletin, v. 115, p. 1133–1152, doi: 10.1130/B25215.1.

Retallack, G.J., Jahren, A.H., Sheldon, N.D., Charkrabarti, R., Metzger, C.A., and Smith, R.M.H., 2005, The Permian-Triassic boundary in Antarctica: Antarctic Science, v. 17, p. 241–258, doi: 10.1017/S0954102005002658.

Rubidge, B.S., ed., 1995, Biostratigraphy of the Beaufort Group (Karoo Supergroup): Biostratigraphic Series, South African Committee for Stratigraphy, v. 1, 46 p.

Sheldon, N.D., 2006, Abrupt chemical weathering increase across the Permian-Triassic boundary: Palaeogeography, Palaeoclimatology, Palaeoecology, v. 231, p. 315–321, doi: 10.1016/j.palaeo.2005.09.001.

Sheldon, N.D., and Retallack, G.J., 2001, Equation for compaction of paleosols due to burial: Geology, v. 29, p. 247–250, doi: 10.1130/0091-7613(2001)029<0247:EFCOPD>2.0.CO;2.

Sheldon, N.D., and Retallack, G.J., 2002, Low oxygen levels in earliest Triassic soils: Geology, v. 30, p. 919–922, doi: 10.1130/0091-7613(2002)030<0919:LOLIET>2.0.CO;2.

Smith, R.M.H., 1987, Helical burrow casts of therapsid origin from the Beaufort Group (Permian) of South Africa: Palaeogeography, Palaeoclimatology, Palaeoecology, v. 60, p. 155–170, doi: 10.1016/0031-0182(87)90030-7.

Smith, R.M.H., 1990, Alluvial paleosols and pedofacies sequences in the Permian Lower Beaufort Group of the southwestern Karoo Basin, South Africa: Journal of Sedimentary Petrology, v. 60, p. 155–170.

Smith, R.M.H., 1993a, Vertebrate taphonomy of Late Permian floodplain deposits in the southwestern Karoo Basin of South Africa: Palaios, v. 8, p. 45–67.

Smith, R.M.H., 1993b, Sedimentology and ichnology of floodplain paleosurfaces in the Beaufort Group (Late Permian), Karoo Sequence, South Africa: Palaios, v. 8, p. 339–357.

Smith, R.M.H., 1995, Changing fluvial environments across the Permian-Triassic boundary in the Karoo Basin, South Africa, and possible causes of the extinctions: Palaeogeography, Palaeoclimatology, Palaeoecology, v. 117, p. 81–104, doi: 10.1016/0031-0182(94)00119-S.

Soil Survey Staff, 2000, Keys to Soil Taxonomy: Blacksburg, Virginia, Pocahontas Press, 600 p.

Stanley, S.M., and Yang, X., 1994, A double mass extinction at the end of the Paleozoic era: Science, v. 266, p. 1340–1344.

Stapleton, R.P., 1978, Microflora from a possible Permo-Triassic transition in South Africa: Review of Palaeobotany and Palynology, v. 25, p. 253–258, doi: 10.1016/0034-6667(78)90029-5.

Stear, W.M., 1980, Channel sandstone and bar morphology of the Beaufort Group uranium district near Beaufort West: Geological Society of South Africa Transactions, v. 83, p. 391–398.

Steiner, M.B., Eshet, Y., Rampino, M.R., and Schwindt, D.M., 2003, Fungal abundance spike and the Permian-Triassic boundary in the Karoo Supergroup (South Africa): Palaeogeography, Palaeoclimatology, Palaeoecology, v. 194, p. 405–414, doi: 10.1016/S0031-0182(03)00230-X.

Stollenhofen, H., Stanistreet, I.G., Rohn, R., Holzfoerster, F., and Wanke, A., 2000, The Gai-As Lake System, southern Namibia and Brazil, *in* Gierlowski-Kordesch, E.H., and Kelts, R.R., eds., Lake Basins Through Space and Time: Tulsa, American Association of Petroleum Geologists, p. 87–108.

Tewari, R., 1996, Paleobotanical investigations from the Raniganj Formation of Jharia Coalfield, *in* Tiku, ed., Gondwana Nine, Volume 1: Rotterdam, A.A. Balkema, p. 135–142.

Thackeray, J.F., van der Merwe, N.J., Lee-Thorp, J.A., Sillen, A., Lanham, J.L., Smith, R., Keyser, A., and Monteiro, P.M.S., 1990, Changes in carbon isotope ratios in the Late Permian recorded in therapsid tooth apatite: Nature, v. 347, p. 751–753, doi: 10.1038/347751a0.

Truswell, E.M., 1980, Permo-Carboniferous palynology of Gondwanaland; progress and problems in the decade to 1980: Bureau of Mineral Resources Journal of Australian Geology and Geophysics, v. 5, p. 95–111.

Visscher, H., Brinkhuis, K., Dilcher, D.L., Elsik, W.C., Eshet, Y., Looy, C., and Traverse, A., 1996, The terminal Paleozoic fungal event: Evidence of terrestrial ecosystem destabilization and collapse: United States National Academy of Sciences Proceedings, v. 93, p. 2135–2158.

Wang, W., Cao, C.-Q., and Wang, Y., 2004, The carbon isotope excursion on GSSP candidate section of Lopingian-Guadalupian boundary: Earth and Planetary Science Letters, v. 220, p. 57–67, doi: 10.1016/S0012-821X(04)00033-0.

Ward, P.D., Montgomery, D.R., and Smith, R.M.H., 2000, Altered river morphology in South Africa related to the Permian-Triassic extinction: Science, v. 289, p. 1740–1743, doi: 10.1126/science.289.5485.1740.

Ward, P.D., Botha, J., Buick, R., de Kock, M.O., Erwin, D.H., Garrison, G., Kirschvink, J., and Smith, R., 2005, Abrupt and gradual extinction among Late Permian vertebrates in the Karoo Basin, South Africa: Science, v. 307, p. 709–714, doi: 10.1126/science.1107068.

Wignall, P., Thomas, B., Willink, R., and Watling, J., 2004, Is Bedout an impact crater? Take 1: Science, v. 306, p. 609–610, doi: 10.1126/science.306.5696.609d.

Zhou, M., Malpas, J., Song, X.-Y., Robinson, P.T., Min, S., Kennedy, A.K., Lesher, C.M., and Keays, R.R., 2002, A temporal link between the Emeishan large igneous province (SW China) and the end-Guadalupian mass extinction: Earth and Planetary Science Letters, v. 196, p. 113–122, doi: 10.1016/S0012-821X(01)00608-2.

Geological Society of America Bulletin

Middle-Late Permian mass extinction on land

Gregory J. Retallack, Christine A. Metzger, Tara Greaver, A. Hope Jahren, Roger M.H. Smith and
Nathan D. Sheldon

Email alerting services	click www.gsapubs.org/cgi/alerts to receive free e-mail alerts when new articles cite this article
Subscribe	click www.gsapubs.org/subscriptions/ to subscribe to Geological Society of America Bulletin
Permission request	click http://www.geosociety.org/pubs/copyrt.htm#gsa to contact GSA

Notes

Geological Society of America